Supplementary information

Poly(N-isopropylacrylamide) Derived Nanogels Demonstrated Thermosensitive Self-assembly and GSH-triggered Drug Release for Efficient Tumor Therapy

Jiaojiao Chen,[a,b] Ming Wu,[a] Hanitrarimalala Veroniaina,[a] Subhankar Mukhopadhyay,[a] Juequan Li,[a] Ziheng Wu ,[c] Zhenghong Wu ,[a] and Xiaole Qi *[a]*

[a] Key Laboratory of Modern Chinese Medicines, China Pharmaceutical University, Nanjing 210009, PR China.

[b] Yantai Yuhuangding Hospital,Yantai 264000, PR China.

[c] Parkville campus, Monash University, VIC 3052, Australia.

Correspondence: Zhenghong Wu; Xiaole Qi

Corresponding author at: Key Laboratory of Modern Chinese Medicines, China Pharmaceutical University, Nanjing 210009, PR China

Tel: +0086-15062208341; Fax: +0086-025-83179703

Email: zhenghongwu66@cpu.edu.cn (Z. H. Wu); qixiaole523@cpu.edu.cn (X. L. Qi)

Table S1. Characteristics of DOX-loaded H-SS-P nanogels. Data are represented as mean ± standard deviation (SD) (n = 3).

Drug/polymer (w/w)	Mean diameter (nm)	Zeta potential (mV)	Encapsulation Efficiency (%)	Drug Loading (%)
0	119.4 ± 1.1	-17.1 ± 0.5	--	--
0.2	130.4 ± 1.9	-23.9 ± 0.6	81.71 ± 0.55	13.62 ± 0.23
0.4	134.3 ± 3.2	-20.8 ± 0.3	75.53 ± 0.55	21.58 ± 0.23
0.6	141.3 ± 2.7	-15.2 ± 0.7	63.17 ± 1.07	23.69 ± 0.58

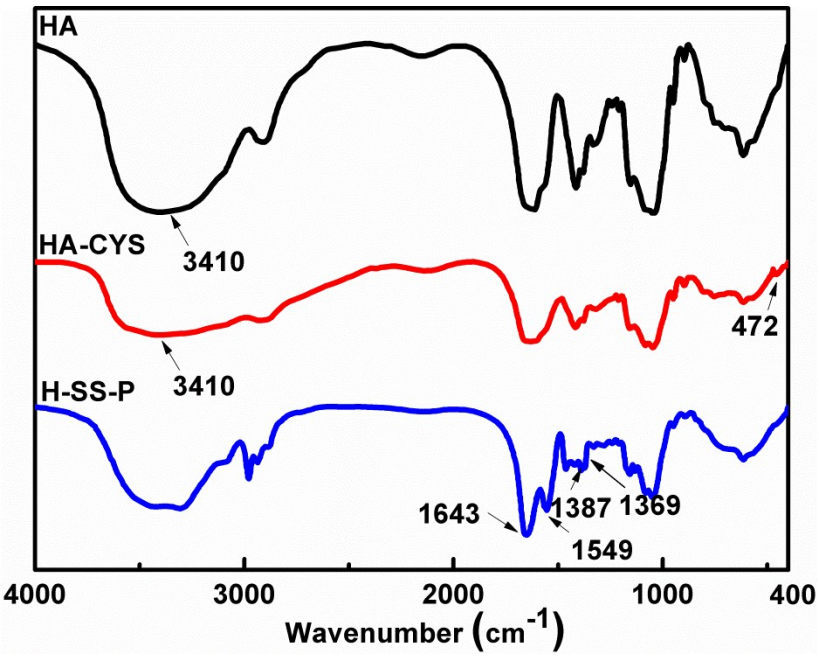

Fig. S1. FT-IR spectra of HA, HA-CYS and HA-SS-PNIPAAm in the wavenumber region of 400-4000 cm^{-1}.

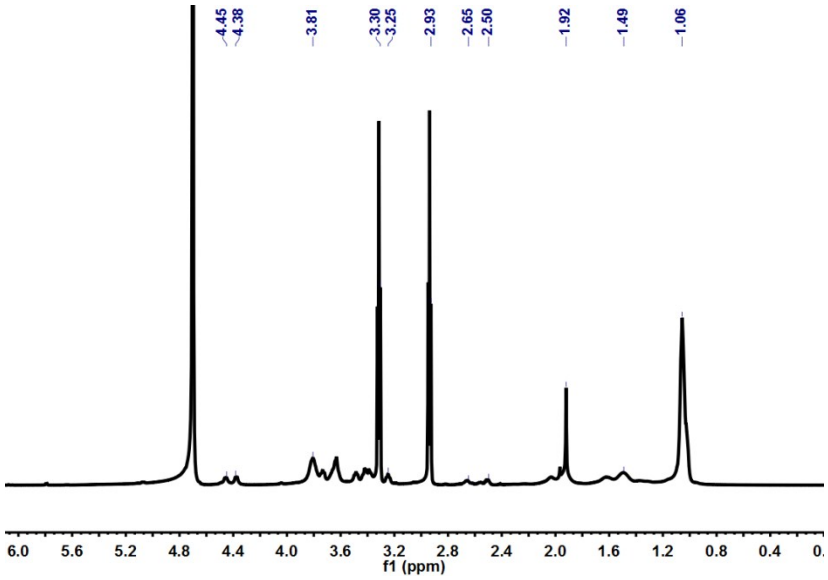

Fig. S2. ^{1}H NMR of a simple mixture of HA, CYS, and PNIPAAm. All compounds were dissolved in D_2O.

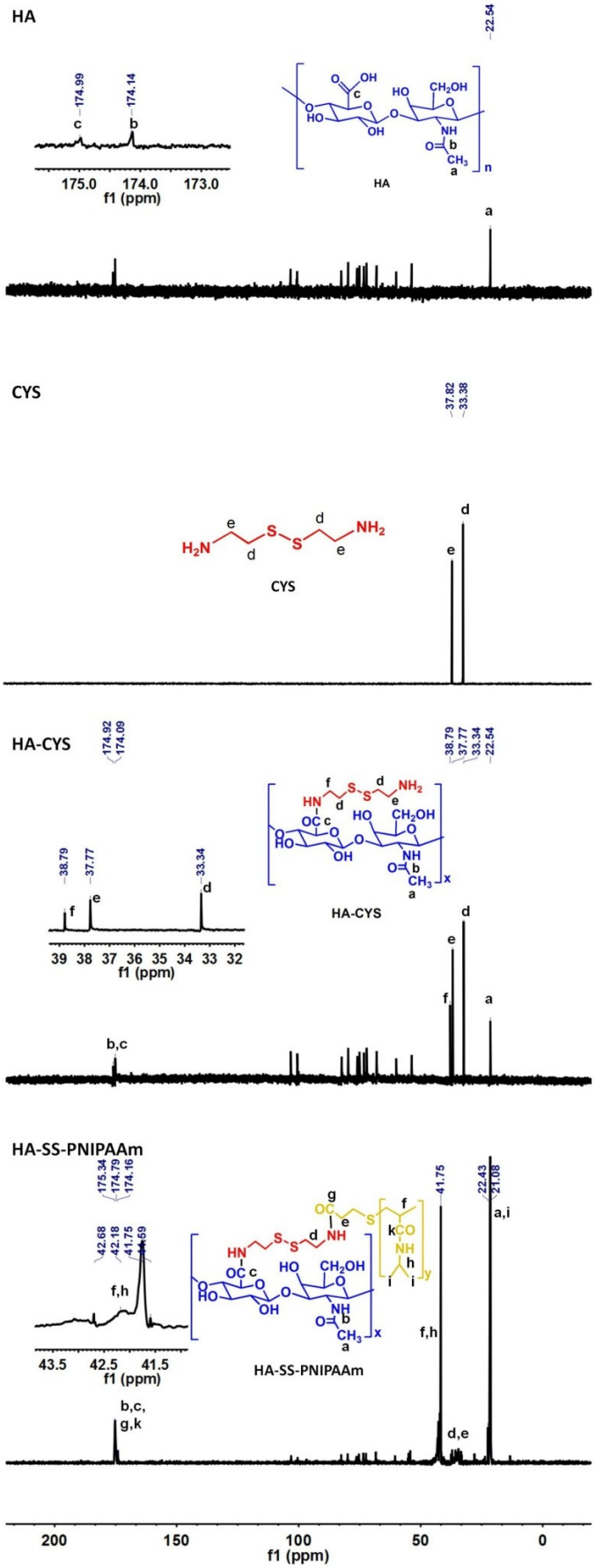

Fig. S3. ^{13}C NMR of HA, CYS, HA-CYS and HA-SS-PNIPAAm. All polymers were dissolved in D_2O.

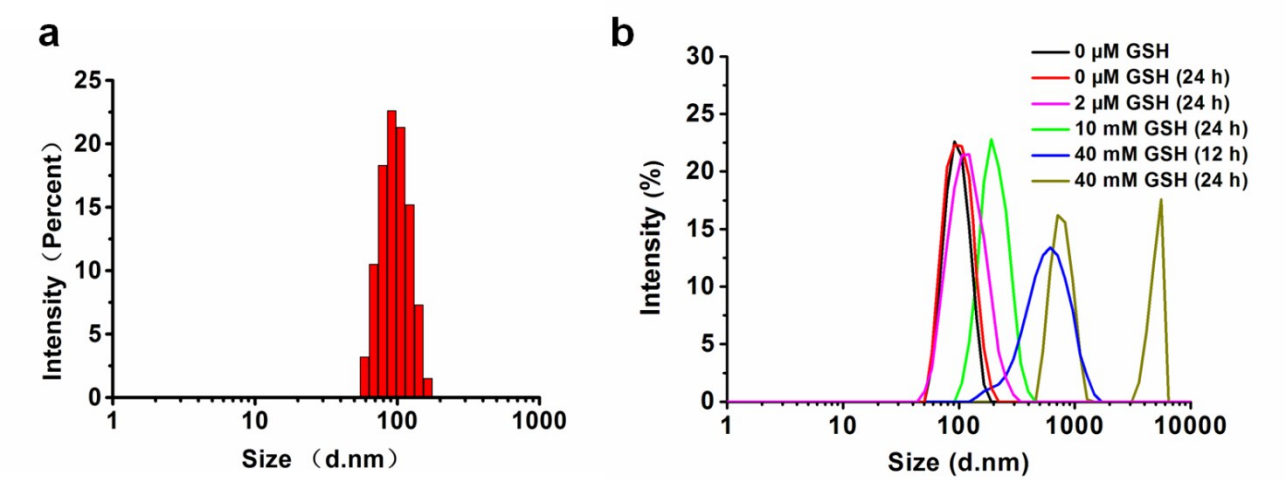

Fig. S4. a) Size distribution of H-SS-P nanogels at 37 °C determined by DLS. b) Size distribution of H-SS-P nanogels in response to GSH at 37 °C determined by DLS. ($MW_{PNIPAAm}$ = 2000 Da, DS 40, C = 0.2 mg/mL)

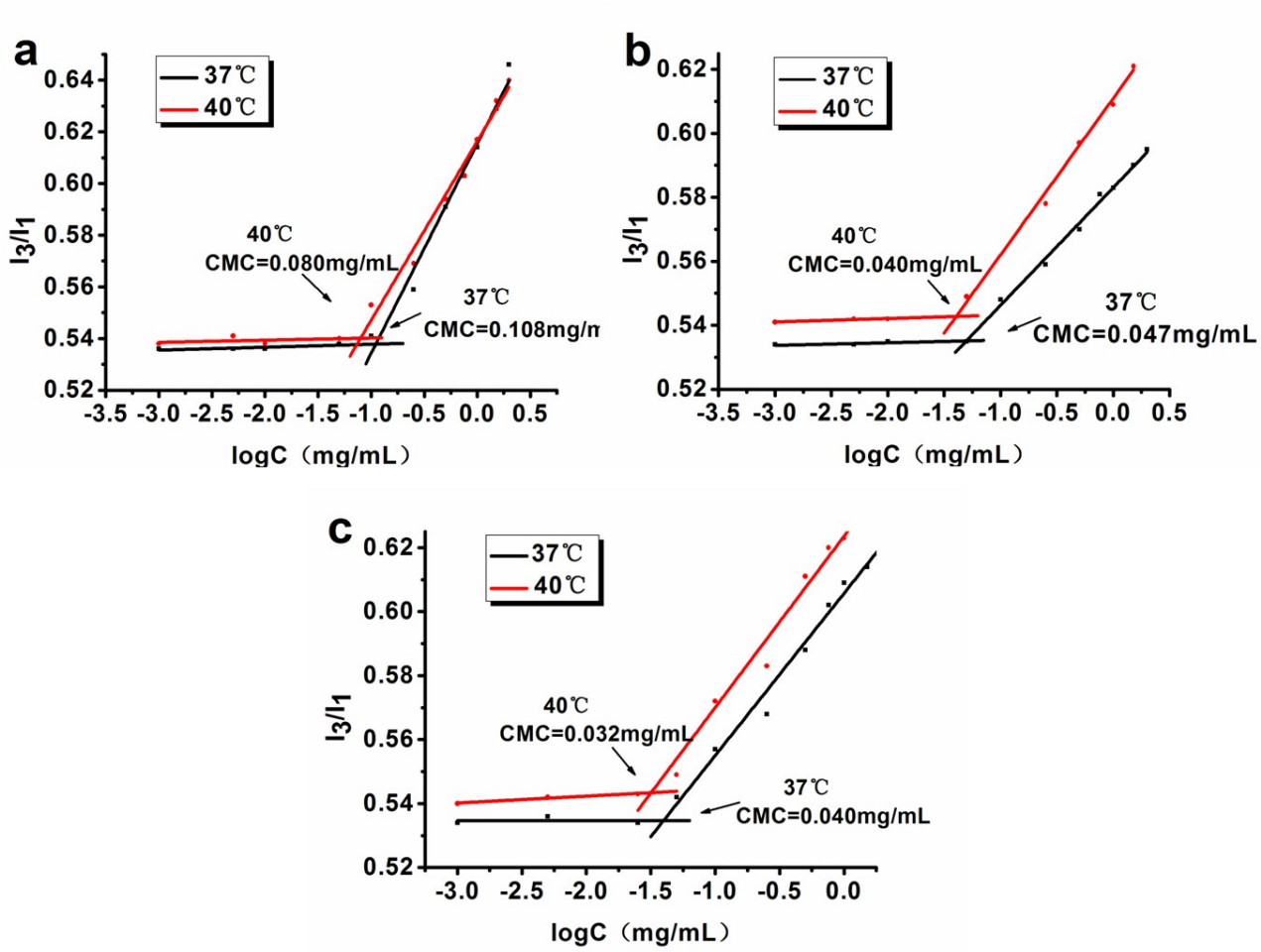

Fig. S5. Critical micelle concentration (CMC) determination of H-SS-P nanogels. a) MW $_{PNIPAAm}$ = 2000, DS20. b) MW $_{PNIPAAm}$ = 2000, DS30. c) MW $_{PNIPAAm}$ = 2000, DS40.

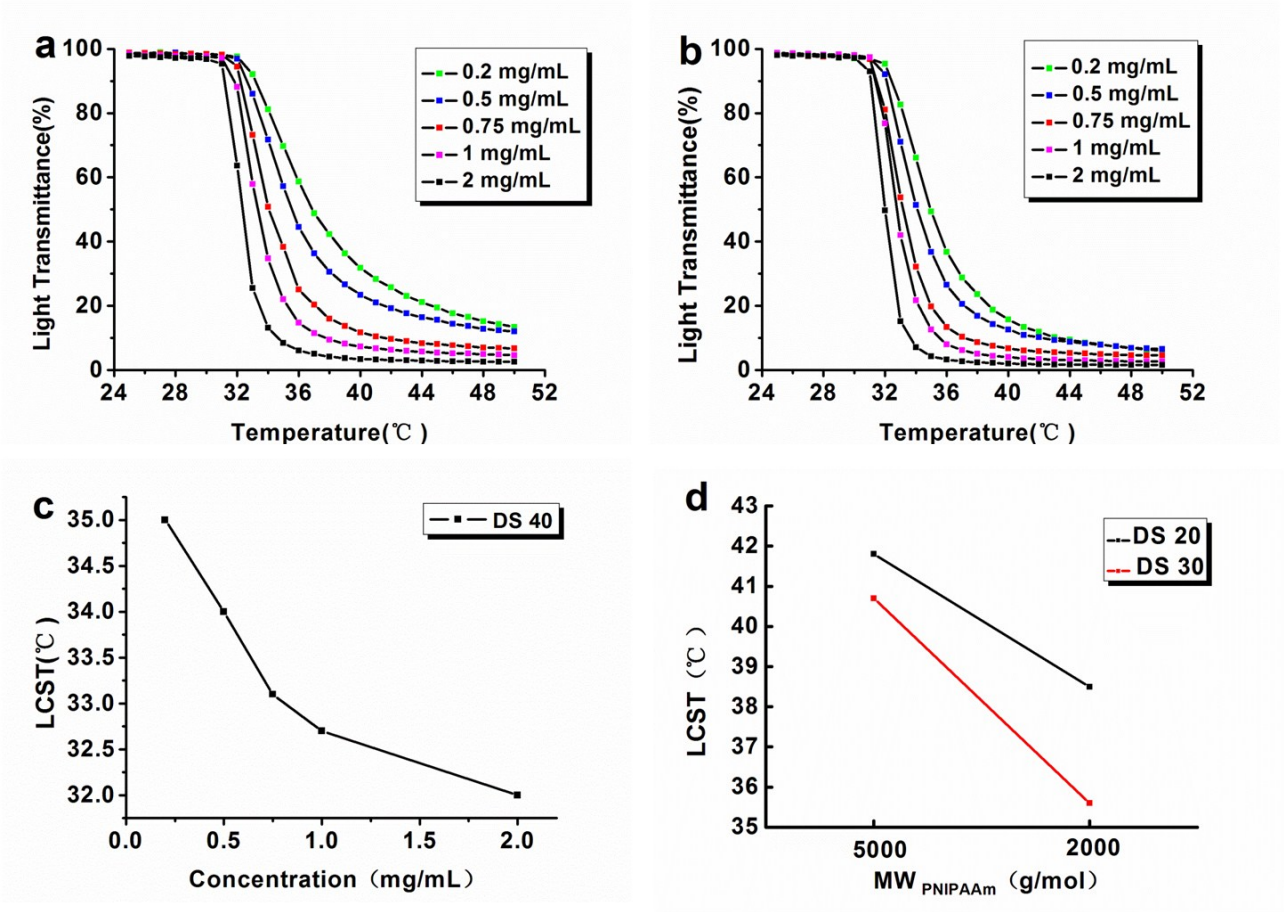

Fig. S6. The results of the lower critical solution temperature (LCST). a) Temperature-transmittance curves of H-SS-P ($MW_{PNIPAAm}$ = 2000, DS30). b) Temperature-transmittance curves of H-SS-P ($MW_{PNIPAAm}$ = 2000, DS40). c) Changes in the LCST with the concentration ($MW_{PNIPAAm}$ = 2000, DS40). d) Changes in the LCST with the number average molecular weight of PNIPAAm-COOH ($MW_{PNIPAAm}$ = 2000, DS40, C = 0.5 mg/mL)

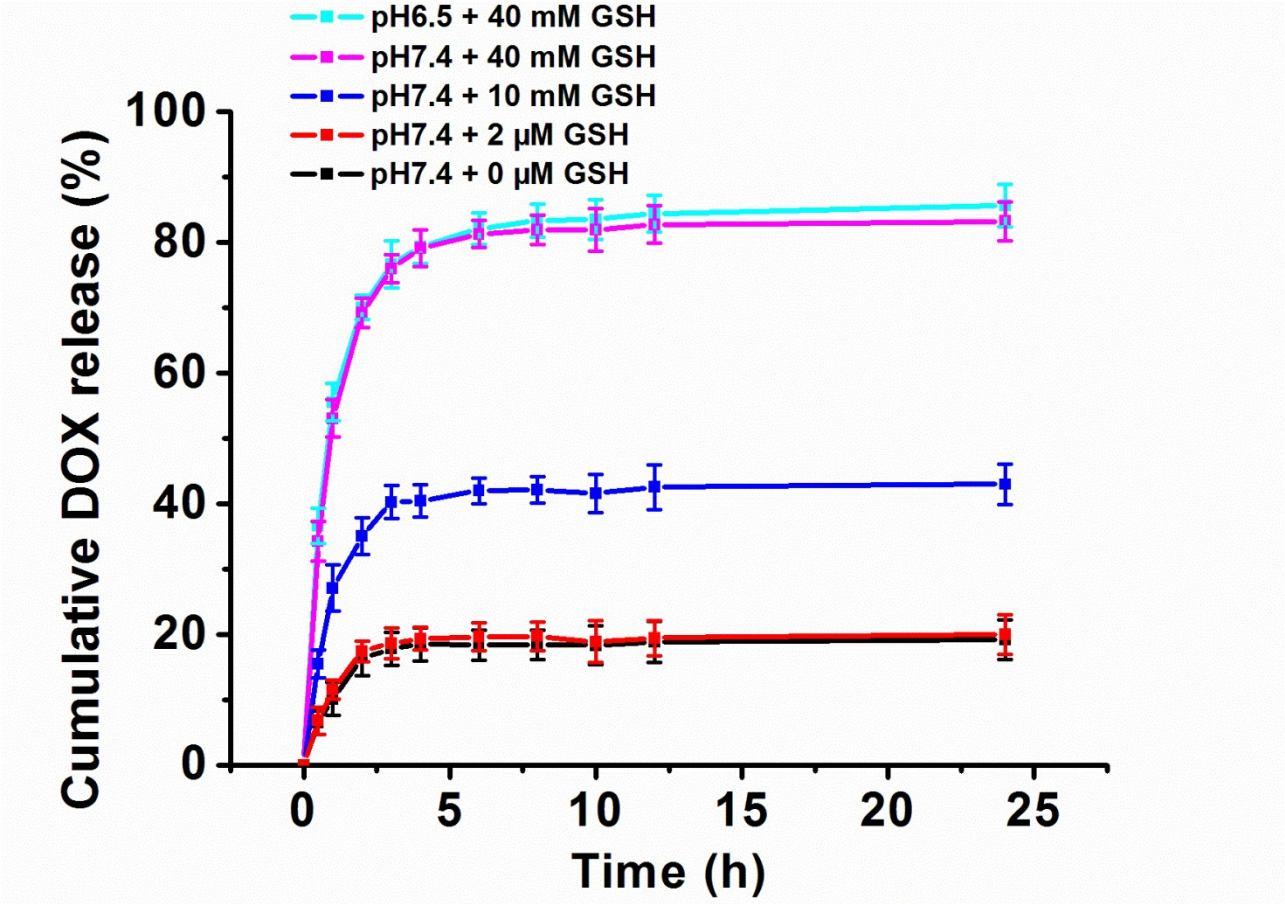

Fig. S7. *In vitro* release behavior of DOX from H-SS-P nanogels triggered by GSH. Data are presented as means ± SD (n = 3).

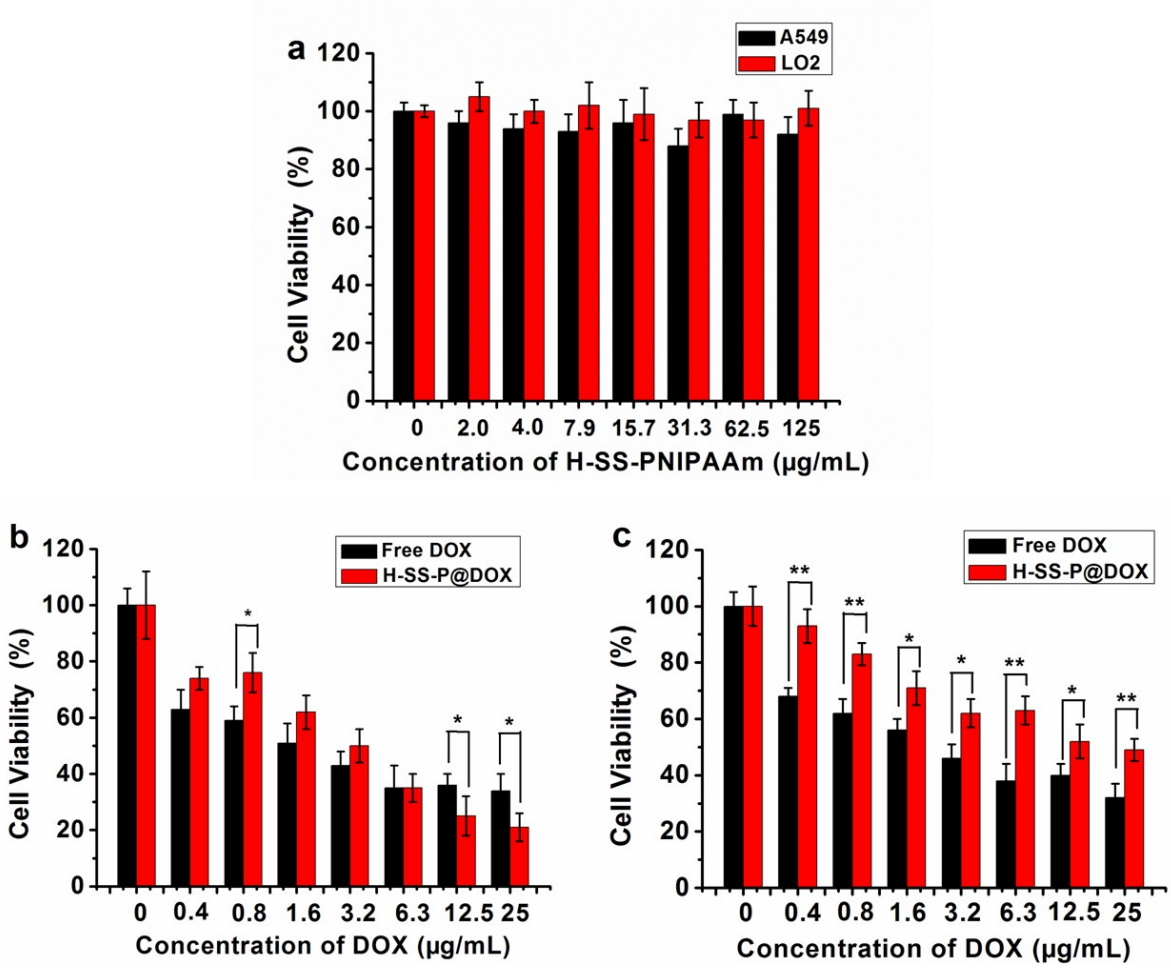

Fig. S8. *In vitro* cytotoxicity of a) blank nanogels against A549 cells and LO2 cells. *In vitro* cytotoxicity of free DOX and H-SS-P@DOX nanogels against b) A549 cells and c) LO2 cells. * and ** represent $p < 0.05$ and $p < 0.01$ vs H-SS-P@DOX group, respectively. Data are presented as means ± SD (n = 3).

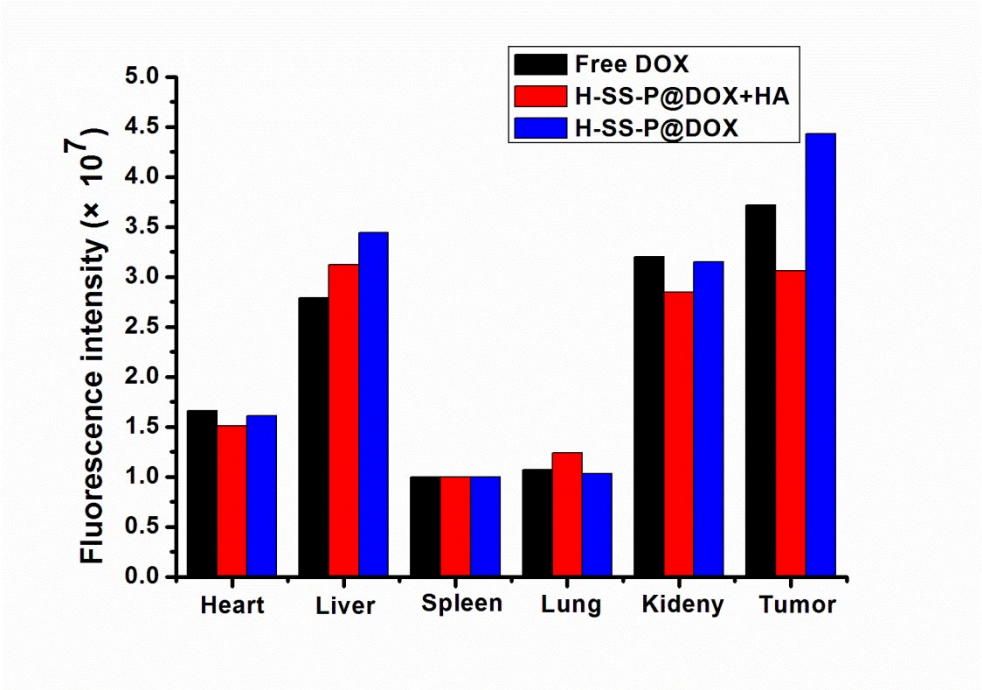

Fig. S9. Quantification of DOX signal for the *in vivo* fluorescence microscopy images of the major organs (heart, liver, spleen, lung and kidney) and tumors in 4T1 tumor-bearing mice after intravenous injection of DOX (control), H-SS-P@DOX with free HA pretreatment and H-SS-P@DOX.

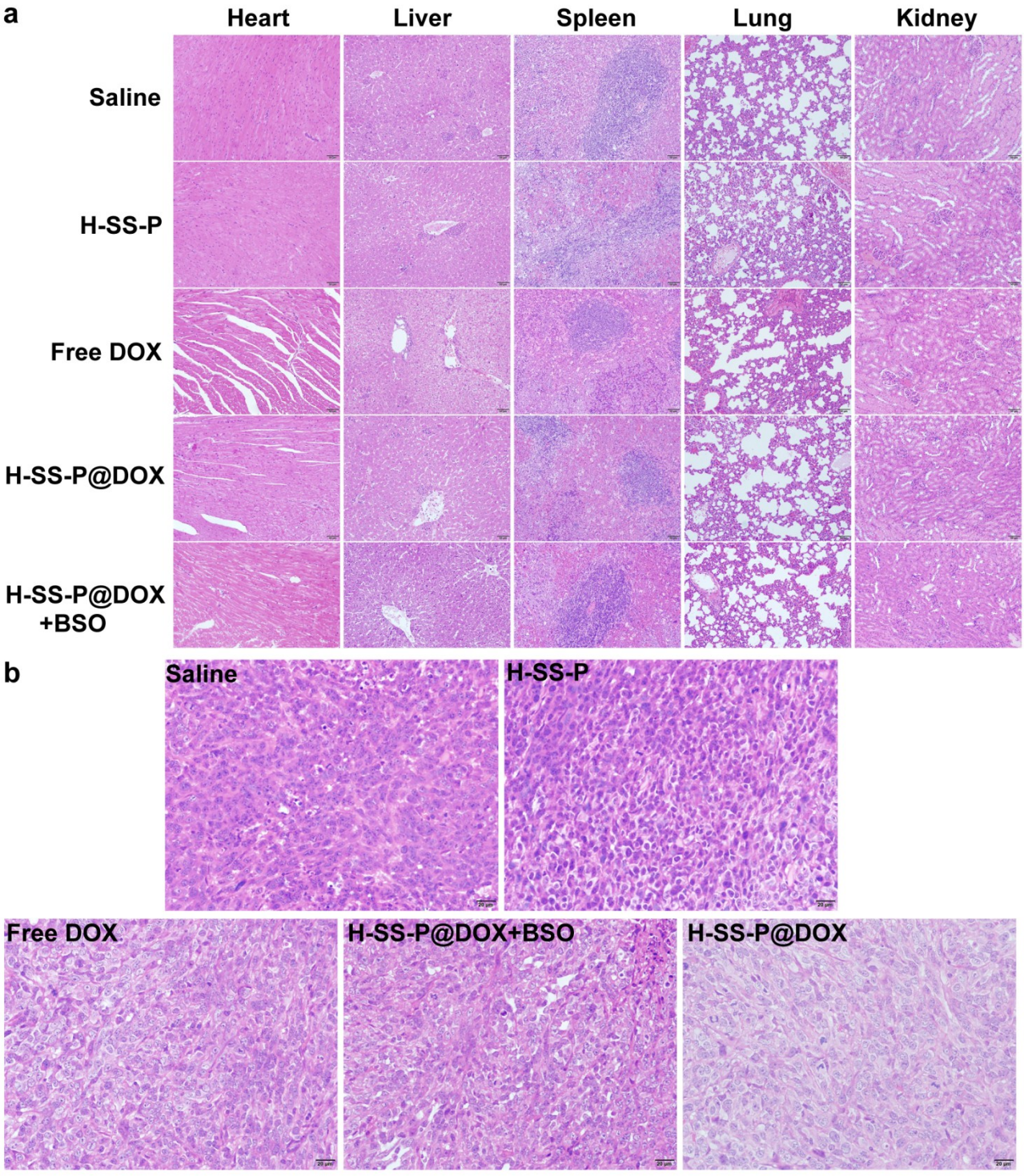

Fig. S10. Histological analysis of a) major organs (heart, liver, spleen, lung and kidney) and b) tumors from 4T1 tumor-bearing mice on the 11th day after they are treated with saline, H-SS-P, free DOX, H-SS-P@DOX and H-SS-P@DOX with BSO treatment.